

## EVIDENCE FOR AN IONIZED REPROCESSOR IN NGC 6814

T. JANE TURNER,<sup>1</sup> CHRISTINE DONE,<sup>2</sup> RICHARD MUSHOTZKY, AND GREG MADEJSKI<sup>1</sup>  
 Laboratory for High Energy Astrophysics, NASA/Goddard Space Flight Center, Greenbelt, MD 20771

AND

HIDEYO KUNIEDA

Department of Astrophysics, Nagoya University, Nagoya, Japan

Received 1991 July 15; accepted 1991 November 5

### ABSTRACT

We report a detailed spectroscopic analysis of a *Ginga* observation of the Seyfert galaxy NGC 6814. We show that the X-ray data are consistent with a scenario in which the continuum radiation is reprocessed in a highly ionized medium, which can either be an accretion disk or a shell of absorbing material. Both of these can produce the strong observed iron  $K\alpha$  line, which must originate within 200 lt-sec of the continuum source. Significant iron  $K\beta$  and nickel  $K\alpha$  are predicted, based on the iron  $K\alpha$  line strength, and these lines partially conceal the iron edge in this source. The spectral variability below  $\sim 4$  keV, where the apparent absorption increases as the continuum flux decreases, is probably caused by a warm absorber covering the reprocessing system.

*Subject headings:* accretion, accretion disks — galaxies: individual (NGC 6814) — galaxies: Seyfert — X-rays: galaxies

### 1. INTRODUCTION

NGC 6814, a low-luminosity Seyfert galaxy ( $L_x \sim 10^{41-43}$  ergs  $s^{-1}$ ), was discovered to exhibit rapid X-ray variability in the *HEAO* A-2 data, with a time scale of  $\sim 100$  s (Tennant et al. 1981). X-ray flares were observed in a long (1 day) *EXOSAT* observation, and a period of 12,000 s was suggested for these events (Mittaz & Branduardi-Raymont 1989; Fiore, Massaro, & Barone 1992a).

A 3 day observation of NGC 6814 was made with the Large Area Proportional Counter (LAC) on the Japanese X-ray astronomy satellite *Ginga* over the period 1989 April 28–30, covering the energy range 1.5–37 keV. A preliminary analysis of these data showed rapid and chaotic variations (up to a factor of 5) throughout the observation (Kunieda et al. 1990, hereafter K90). As reported by K90 and Turner et al. (1991), the flat spectral index ( $\alpha \sim 0.4$ ), and large equivalent width ( $W_\alpha$ ) of the iron  $K\alpha$  line ( $\sim 350$  eV) are not consistent with the spectra seen in the majority of Seyfert galaxies (Pounds et al. 1990). In these data, the line equivalent width is typically  $\sim 100$  eV, and the observed spectral index is  $\sim 0.7$  in the 2–20 keV range, where both of these properties can be explained in the context of X-ray illumination of the accretion disk by an intrinsic power law of  $\alpha \sim 0.9$ . [Throughout this paper, we define the power-law index  $\alpha$  such that flux density  $S(E)$  depends on energy  $E$  via  $S(E) \propto E^{-\alpha}$ .] From their spectral fits to the *Ginga* NGC 6814 data, Turner et al. (1991) give a best-fit value with no reflection component, with 90% confidence upper limit on the subtended solid angle  $\Omega/2\pi$  of the cold reflecting material of 0.8 (one interesting parameter) for a face-on disk. The zero value of best fit of  $\Omega/2\pi$  is primarily due to an absence of the predicted iron K-edge in the data.

A further surprising result from this observation is that the line and continuum flux were correlated throughout the rapid

variability (K90), indicating that the difference in light travel path for the line and continuum photons is small. Here we show the results of a more detailed spectral analysis of NGC 6814, including the discussion of the absorption variability and anticorrelation of the intrinsic absorption with the flux level, as well as the shape of the iron line. From our spectral fits, we infer that the *Ginga* data can be described by a reflection of the continuum source from a medium containing highly ionized material, which is in fact expected given the proximity of the ionizing continuum to the reprocessor. The detailed discussion of the X-ray variability, including the search for periodicity in the unevenly sampled *Ginga* data, is presented in a separate paper (Done et al. 1992b; see also Done et al. 1991a and Done et al. 1991b). Some results from the timing paper are given here, as appropriate to the interpretation of the spectral data.

### 2. INITIAL DATA REDUCTION

A set of conservative data rejection criteria were applied to achieve a maximum signal to noise, whilst eliminating data taken in high background sections of the *Ginga* orbit (related to the South Atlantic Anomaly). Solar contamination was avoided by rejecting data when the Sun angle was  $< 90^\circ$  (see Makino et al. 1987 and Hayashida et al. 1989). For background subtraction we applied a method described in Turner et al. (1989), using background data obtained 2 days prior to the observation of NGC 6814. Since the addition of data from the LAC mid-layer detectors did not improve the signal-to-noise ratio, for spectral fitting reported here we just used top layer data. As it was difficult to completely remove the radioactive decay line feature at  $\sim 5$  keV, we excluded the affected channels (7–9) from this analysis. The only data presented here are those taken when the spacecraft was pointing within  $0^\circ.1$  of the source. Within this specification, spectral contamination from collimator reflection is  $< 1\%$  for low energies ( $< 3$  keV) and negligible at higher energies. A 0.5% systematic error on the net (background subtracted) counts has been included in the spectral data files.

<sup>1</sup> Universities Space Research Association.

<sup>2</sup> NAS/NRC Resident Research Associate.

### 3. RESULTS

The data from the whole observation was split into four intensity states as described in K90 to obtain further information on the source behavior than can be gathered from the mean spectrum. These four spectra are all adequately fitted by a power law absorbed by cold gas with Galactic abundances and cross sections given in Morrison & McCammon (1983), and narrow Gaussian line as detailed in K90. The spectral index is constant to within the errors and is very flat with  $\alpha = 0.4$  (weighted mean). Table 1 shows the parameters for the high state spectrum, for which there is the best signal-to-noise ratio.

#### 3.1. Absorption

The column density is considerably greater than the galactic column in the line of sight of  $0.98 \times 10^{21} \text{ cm}^{-2}$  (Elvis, Lockman, & Wilkes 1989), indicating the presence of a substantial intrinsic absorption in NGC 6814. The 90% confidence ranges in column density for the four intensity-selected spectra (K90) are inconsistent with each other, so this *intrinsic column* is also *variable*. Figure 1 shows the hardness ratio (3–5.5 keV/1.5–3.0 keV) versus the 7–20 keV count rates. There is a correlation (significant at >99% confidence) in the sense that the absorption increases as the power-law intensity decreases. We can exclude a selection effect, whereby the count rate decreases *due* to this increase in absorption, as the effect of the absorption is negligible above 7 keV.

A change in a cold absorption column correlated with source intensity seems contrived. A much more physically appealing solution is that the change in the apparent column density is due to the increased level of ionization of the absorber by the central source, and thus decrease in the opacity; during the high state of the source, the gas is partially ionized. This behavior has been seen in other AGNs (Halpern 1984; Fiore et al. 1992b). However, the partially ionized (warm) absorber *alone* cannot explain the NGC 6814 data, as discussed in § 3.3 below.

#### 3.2. Line Emission

As noted in K90, the Fe K $\alpha$  line, when fitted with a narrow Gaussian profile, has a constant equivalent width  $W_\alpha$  of  $\sim 350$

TABLE 1

GAUSSIAN LINE FITS FOR NGC 6814

Parameter	Narrow Line	Broad Line
Power-law index $\alpha$ .....	$0.49 \pm 0.08$	$0.45 \pm 0.07$
Continuum normalization (photons $\text{s}^{-1} \text{keV}^{-1}$ ) .....	$51.6 \pm 7.5$	$46.7 \pm 9.5$
Column density $N_{\text{H}}$ ( $\times 10^{22} \text{ cm}^{-2}$ ) .....	$4.37 \pm 0.38$	$4.05 \pm 0.40$
Line energy (keV) .....	$6.37 \pm 0.14$	$6.28 \pm 0.13$
Line normalization (photons $\text{s}^{-1}$ ) .....	$0.94 \pm 0.18$	$1.23 \pm 0.43$
Intrinsic width of the line rms (keV) .....	0.05 (fixed)	0.40 (+0.3, -0.4)
Equivalent width of the line (eV) .....	$355 \pm 55$	$381 \pm 125$
$\chi^2$ (21 d.o.f.) .....	15.1	13.6

NOTES.—The spectral data presented here are for the highest flux state of the source (where the 2.3–20 keV flux is  $11.3 \pm 1.1 \times 10^{-11} \text{ ergs cm}^{-2} \text{ s}^{-1}$ ; see Kunieda et al. 1990). The normalizations for both the power law and line are obtained with an effective area of  $4000 \text{ cm}^2$ . Errors are 90% confidence for one interesting parameter.

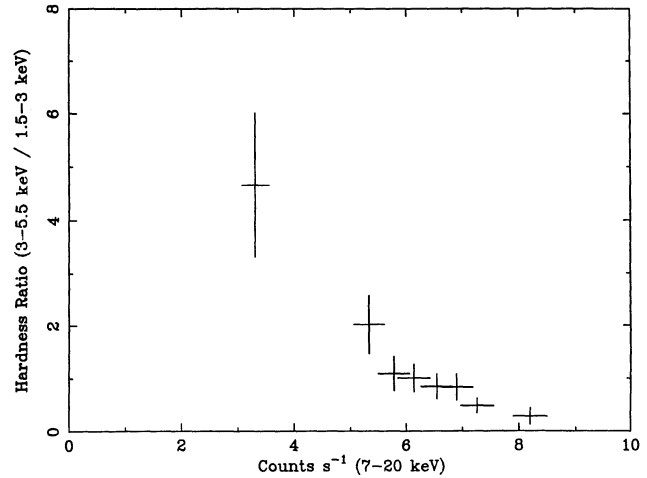


FIG. 1.—Hardness ratio (3–5.5 keV/1.5–3.0 keV) as a function of the source counting rate (7–20 keV) showing the inverse correlation between the source flux and the intrinsic absorption.

eV in all four intensity-selected spectra, implying that the line and continuum intensity are well correlated. A *broad* Gaussian model, preferred at 75% confidence in the best signal-to-noise ratio data (Table 1), yields  $W_\alpha = 381 \pm 125 \text{ eV}$  (as the shallower line profile coupled with the poor spectral resolution of the proportional counter detectors includes more photons in the line). The line energies for both the narrow line,  $6.37 \pm 0.14 \text{ keV}$  (90% confidence), and the broad line,  $6.28 \pm 0.13 \text{ keV}$ , are consistent with the 6.4 keV expected from cold iron fluorescence K $\alpha$  emission. The mean line-of-sight column of  $5 \times 10^{22} \text{ cm}^{-2}$  should produce an equivalent width of only 30 eV if the material is distributed spherically around the X-ray source (Inoue 1989) with solar abundances of elements. This is an order of magnitude below the observed line intensity, ruling out the cold column as the origin of the line.

As a consequence of the high iron K $\alpha$  line strength in this source, we expected a significant contribution of flux from an iron K $\beta$  line and a nickel K $\alpha$  line. The Fe K $\beta$  line has an energy of 7.05 keV in neutral material, and a strength of  $\sim 10\%$  of that of the K $\alpha$  line (Fig. 2; Kikoin 1976). In addition, we expect a Ni K $\alpha$  line emitted at 7.47 keV in neutral material with the equivalent width

$$W(\text{Ni K}\alpha) = W(\text{Fe K}\alpha) \frac{FY(\text{Ni})A(\text{Ni})P_{\text{esc}}(\text{Ni})}{FY(\text{Fe})A(\text{Fe})P_{\text{esc}}(\text{Fe})},$$

where  $FY$  is the fluorescence yield ( $\approx 0.41$  for Ni, and  $\approx 0.34$  for Fe; Bambynek et al. 1972),  $A$  is abundance, and  $P_{\text{esc}}(\text{Fe})$  and  $P_{\text{esc}}(\text{Ni})$  are the escape probabilities at the Fe and Ni line energies, respectively. Assuming that the line originates in a cold accretion disk,  $P_{\text{esc}}(\text{Ni})/P_{\text{esc}}(\text{Fe}) \approx 0.85$  (from Fig. 2 of Lightman & White 1988). We assume an iron/nickel abundance ratio of 16:1, though we note that this may be an underestimate (Halpern & Oke 1986). In a “typical” AGN in which the equivalent width of the Fe K $\alpha$  line is 100 eV, the predicted Fe K $\beta$  line is only 11 eV and that of the Ni K $\alpha$  line is  $\sim 5 \text{ eV}$ , completely undetectable in *Ginga*. On the other hand, for NGC 6814 the minimum equivalent width of the Fe K $\beta$  and Ni K $\alpha$  lines (for a simple power law and a narrow Fe K $\alpha$  line) is 36 and 18 eV, respectively. Any spectral model for NGC 6814 must then include these lines.

#### 3.3. The Warm Absorber

The cold absorber alone cannot produce the observed line. As the variable absorption observed suggests the presence of a

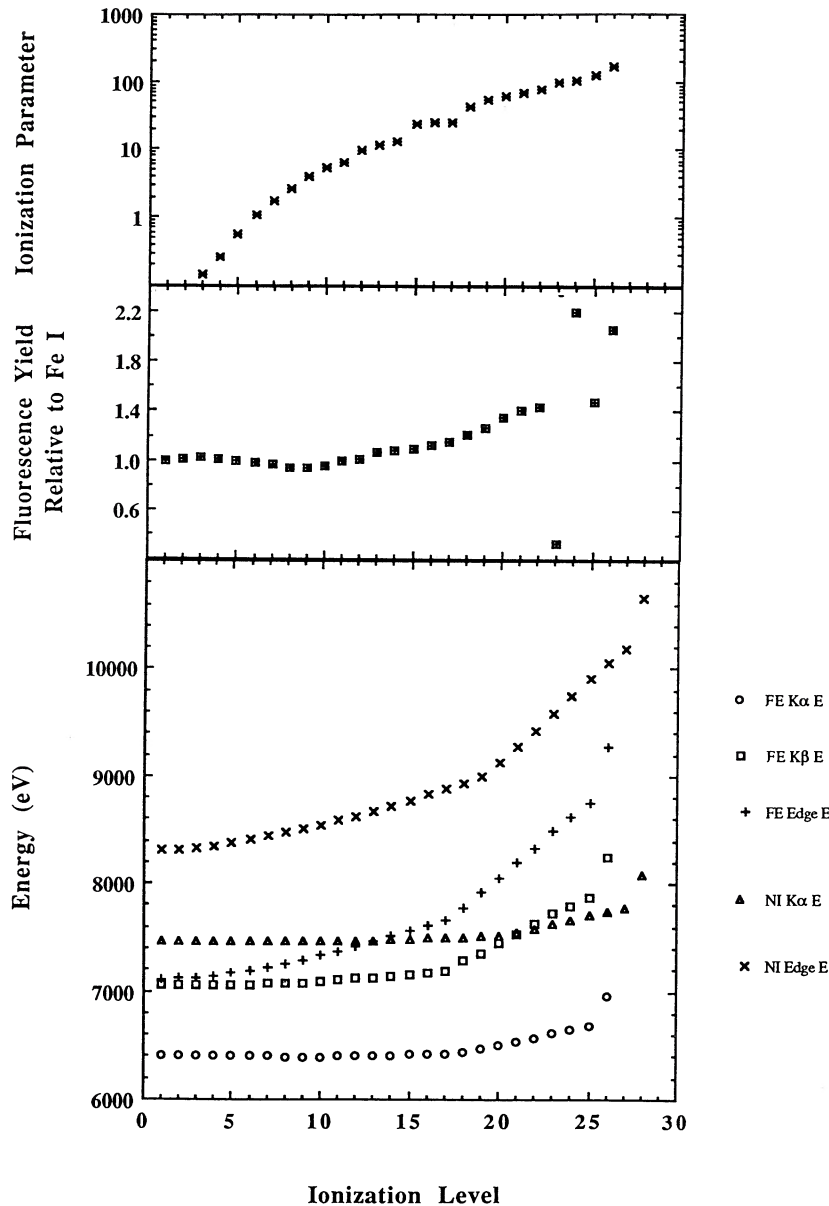


FIG. 2.—*Bottom*: Energies of iron and nickel K edges (from Rielman & Manson 1979), iron and nickel  $K\alpha$  (from House 1969 and Morita & Fujita 1983), and iron  $K\beta$  (from Klapisch et al. 1977 and Morita & Fujita 1983), plotted as a function of the ionization state. *Middle*: Iron fluorescence yield vs. ionization state of iron (from Krolik & Kallman 1987 and Jacobs & Rozsnyai 1986). *Top*: The ionization parameter where the fraction of the given ionization state peaks (from T. Kallman 1991, private communication). Note that this changes with changing input spectrum. We assume a power law from 13.6 eV to 13.6 keV with an energy index  $\alpha = 0.5$ . Key to symbols: *open circles*, Fe  $K\alpha$  E; *open squares*, Fe  $K\beta$  E; *plus signs*, Fe edge E; *filled triangles*, Ni  $K\alpha$  E; *crosses*, Ni edge E.

warm absorber in NGC 6814, we now consider the line arising from such material. Ionization reduces the low-energy opacity of the material from that expected from a cold column, leading to an underestimate of the measured column density. Assuming that the line energy of  $\sim 6.4$  keV is a true indication of the ionization state of the material, this indicates that the absorber is not highly ionized, i.e., that iron is below Fe XVIII, then the associated Fe edge from the absorber must be between 7.1 and 7.7 keV (see Fig. 2). A line with  $W_\alpha = 400$  eV would require  $N_H \sim 4 \times 10^{23}$   $\text{cm}^{-2}$  (cf. Inoue 1989), for a spherical absorber, and thus the model predicts an Fe edge with  $\tau = 0.54$ . From spectral fits, including the Fe  $K\beta$  and Ni  $K\alpha$

lines, with equivalent width of 40 and 20 eV, respectively, the 90% confidence upper limit (Fig. 3a) on the Fe edge between 7.1 and 7.7 keV is  $\tau \approx 0.12$ , ruling out this scenario.

We note that the calculations for the equivalent width by Inoue (1989) apply to cold (neutral) material; as the material becomes more ionized, the opacity at the Fe line energy decreases. Specifically, at the highest ionization stages of Fe, all of the lighter elements are already fully stripped, and the material is nearly completely transparent below the Fe edge. In this simplest case, where the opacity is provided solely by the Fe edge,  $W_\alpha$  of 400 eV requires a column of only  $\approx 2.5 \times 10^{23}$   $\text{cm}^{-2}$  (as compared to  $4 \times 10^{23}$   $\text{cm}^{-2}$  for neutral material,

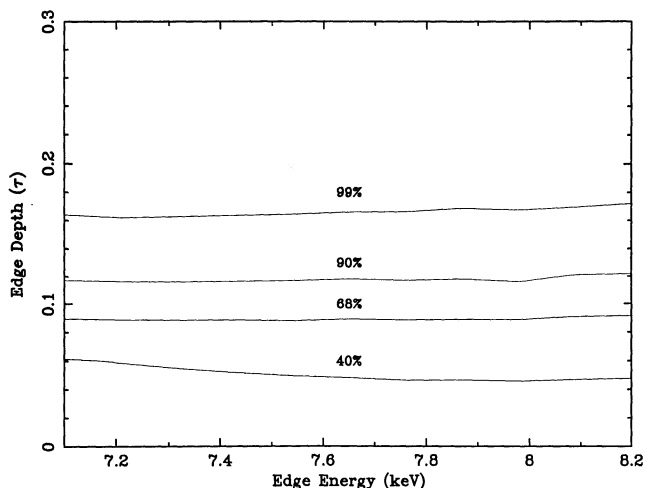


FIG. 3a

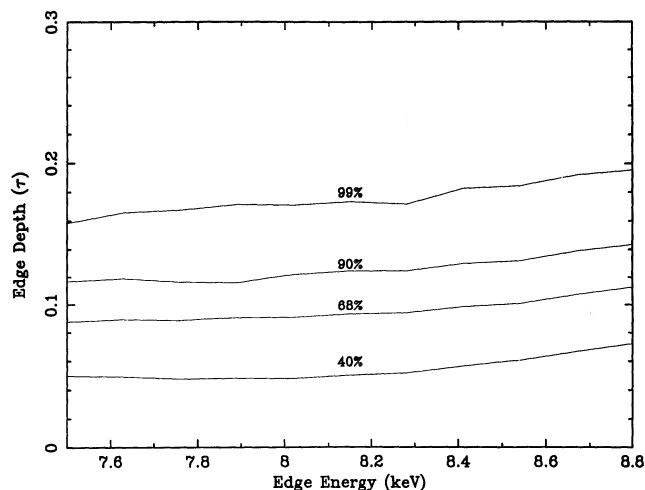


FIG. 3b

FIG. 3.—(a) Confidence contours (40, 68, 90, and 99%) for the optical depth of the iron K edge at all physically relevant energies for cool material (7.1–8.2 keV), corresponding to the  $\xi \leq 50$ , with the Fe K $\beta$  and Ni K $\alpha$  line energies of 7.05 and 7.47 keV, respectively. (b) As (a), but for highly ionized material ( $\xi = 100$ ), with the combined effects of ionization and gravitational redshift giving the Fe K $\alpha$  at 6.3 keV, and Ni K $\alpha$  and Fe K $\beta$  approximated as a blend centered at energy 7.35 keV, for the range of edge energies 7.5–8.8 keV.

where about one-third of the line photons are absorbed). This reduces the required edge to  $\tau \approx 0.34$ , still ruled out by our 90% confidence limit.

For highly ionized material, the fluorescence yield increases by up to a factor of 2 (Krolik & Kallman 1987; see also Fig. 2), with the maximum yield occurring for Fe xxiv. At this ionization stage, the required column must still be  $> 1.25 \times 10^{23} \text{ cm}^{-2}$ , equivalent to an Fe edge with  $\tau = 0.16$ . In this state, the emitted iron line energy is 6.67 keV (Inoue 1989; Makishima 1986), inconsistent with the observed line energy at  $> 90\%$  confidence, thus requiring the line to be redshifted and hence that the absorber be extremely close to the black hole. For the observed line energy of  $6.3 \pm 0.12$  keV, we require a gravitational redshift of  $\sim 6\%$ . This redshift will also affect the energy of the associated Fe K $\beta$  and Ni K $\alpha$  lines from their expected ionized energies of 7.70 and 7.65 keV, such that they both are at  $\sim 7.35$  keV (cf. Fig. 2), and will shift the associated ionized Fe edge from its rest ionized energy of 8.8 keV to  $8.3 \pm 0.15$  keV. The spectrum limits the depth of the edge in this energy range to  $\tau < 0.12$  and  $0.17$  at the 90% and 99% confidence level, respectively (Fig. 3b). We show the marginally consistent solution, with an Fe K edge of depth  $\tau = 0.16$  and energy of 8.3 keV, in Figures 4a–4c. We note, however, that such highly ionized material, in which oxygen is fully stripped, cannot produce the low-energy variability seen in Figure 1. Thus we require that there is a stratification of the ionized material, with a highly ionized absorber to account for the observed Fe line and a warm absorber to give the observed absorption variability with flux. The modeling of this stratified absorber is beyond the scope of this paper.

#### 3.4. An Accretion Disk

X-ray-illuminated accretion disks provide an attractive alternative scenario which seems to work quantitatively for many AGNs (e.g., Pounds et al. 1990; Inoue 1989). The spectral signature of such accretion disks includes an iron line and Compton reflection (Lightman & White 1988; Guilbert & Rees 1988; George & Fabian 1991; Matt, Perola, & Piro 1991). The combination of the decrease in reflection albedo due to

photoelectric absorption at low energies and Compton down-scattering and the reduction of the scattering cross section at high energies give the reflected spectrum a characteristic shape which has a broad peak between 10 and 100 keV. Reflection has two characteristic signatures seen in the *Ginga* 2–30 keV band: first, the iron edge in the reflected spectrum gives a pseudo-edge in the total (direct + reflected) spectrum, and second, the spectrum hardens above 10 keV. Motivated by the presence of the strong Fe K $\alpha$  line in the X-ray spectrum, we examine the applicability of such reflection models to our data.

##### 3.4.1. Iron Line from an Accretion Disk

If the line arises from reprocessing in an accretion disk, then the ordered angular momentum structure imparts a characteristic profile as the line emission from the accretion disk rotating towards the observer is Doppler-boosted and blueshifted, whereas the emission from the opposite side is Doppler-suppressed and redshifted (Fabian et al. 1989; Laor 1991). The asymmetric line profile was fitted to the high-state spectrum alone (since only that spectrum has a sufficient signal-to-noise ratio for a meaningful fit) but was not preferred over the Gaussian line fits. We assumed the line arises in a region of radius 3–50 $R_g$  on the disk, and approximated the line emissivity as a power-law function of radius, of index  $-3$  (see, e.g., Fabian et al. 1989). Table 2 lists disk-line iron K $\alpha$  fits for inclination angles  $\theta$  of  $0^\circ$ ,  $45^\circ$ , and  $70^\circ$ . The mean equivalent width is 776 eV, even larger than for the symmetrical line, as the gradually sloping red wing of the profile includes many more photons even than the broad Gaussian. The low inclination fits are statistically preferred over the  $70^\circ$  fit (at 90% confidence) as the intrinsic line width and line energy become too large and too small, respectively, at high inclinations (see Table 1 and Matt et al. 1991). Thus, if the disk line model is appropriate, the data suggest moderate to low inclination angles.

In order to account for the large  $W_\alpha$  in this scenario, a large solid angle is needed for reprocessing. However, since the line must be produced close to the continuum source, it should arise only from the innermost part of the disk, limiting the

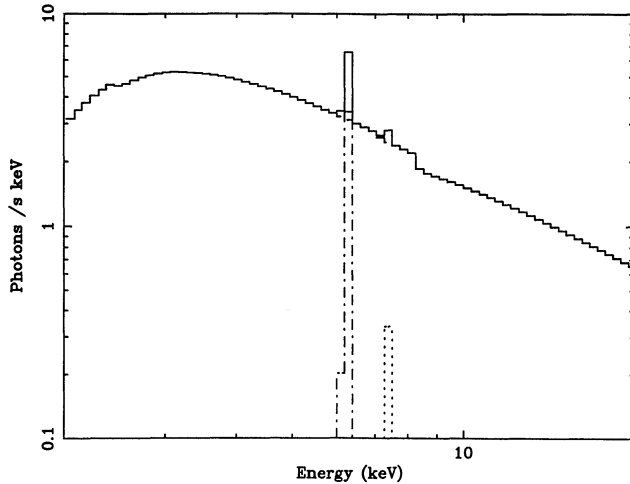


FIG. 4a

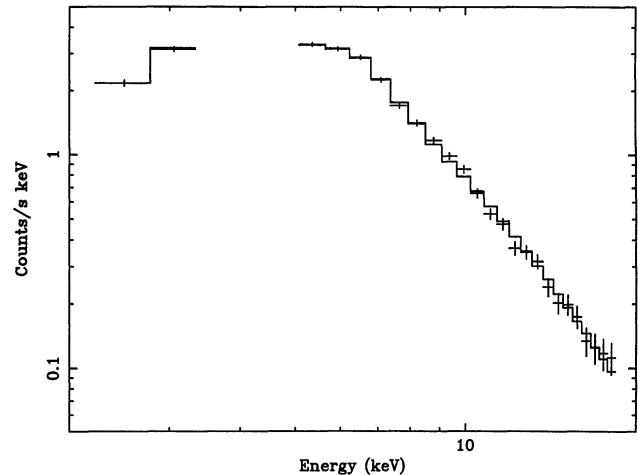


FIG. 4b

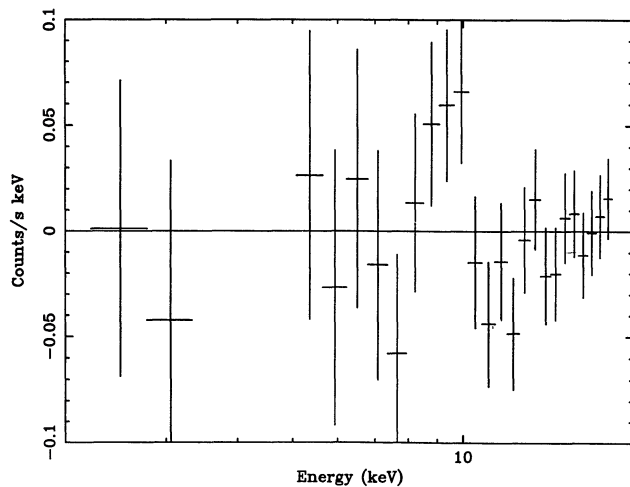


FIG. 4c

FIG. 4.—(a) The marginally self consistent model (1% level) in which the Fe  $K\alpha$  line equivalent width of 350 eV is produced from highly ionized ( $\xi = 100$ ), spherically distributed material close to the black hole. The Fe  $K$  edge depth is fixed to  $\tau = 0.16$  at an energy of 8.3 keV, as appropriate for the redshift required for the line energy. Fe  $K\beta$  and Ni  $K\alpha$  lines are included as given in the text. (b) The *Ginga* data for NGC 6814 and the model illustrated in (a), folded through the detector response. (c) The residuals to the model illustrated in (a).

subtended solid angle for a flat disk geometry, and requiring a steeply peaked line and reflection emissivity. One way to explain this restricted range of radius is if the disk geometry is a funnel, forming the innermost part of a geometrically thick disk. Matt et al. (1991) calculate a maximum equivalent width of 230 eV for an iron line arising from such concave disk geometries, where the reprocessing material is neutral. Alternatively, general relativistic effects can result in the iron line being preferentially observed from the inner regions of the accretion disk when the X-ray source is very close to the black hole horizon (within a few  $R_s$ ; Matt et al. 1991). The flat spectral index increases the expected line equivalent width for a face-on, flat disk from 145 eV ( $\alpha = 0.9$ ) to 177 eV ( $\alpha = 0.5$ ), as there are more photons at high energies to produce the line (George & Fabian 1991). However, the observed  $K\alpha$  line strength is still a factor of 3 greater than that predicted by cold, cosmic abundance accretion disk models.

While there is evidence for an abundance gradient in nearby spiral galaxies such that at the nucleus the heavy element abundances are 2–3 times solar (e.g., Lambert 1989 and references therein), George & Fabian (1991) note that such increased elemental abundances will not significantly increase  $W_\alpha$ . The reason for this is that although there are more line-producing atoms, there are more atoms providing opacity as well, preventing the line photons from escaping the reprocessor. An overabundance of iron alone would allow a significant increase in  $W_\alpha$ ; however, it would also proportionally increase the strength of the iron edge.

Ionization of the reprocessing material also allows an additional increase in  $W_\alpha$  as the opacity to line photons is decreased (as explained in § 3.3). From the 50–200 s lag of the iron line behind the continuum (Done et al. 1991b), the disk may be ionized. With the X-ray luminosity  $L_x \sim 10^{43}$  ergs  $s^{-1}$ , the distance from the ionizing source  $D \sim 10^{13}$  cm (inferred from the line variability constraint), and density  $n > 10^{14}$   $cm^{-3}$  (from a standard Shakura & Sunyaev disk, calculated at 25 Schwarzschild radii ( $= 2GMc^{-2}$ ); cf. Matt et al. (1991), assuming the viscosity parameter  $\alpha < 1$  for a source of  $\sim 10^6 M_\odot$  running at  $\sim 30\%$  of the Eddington limit), we calculate  $\xi$  (defined as  $L_x/nD^2$  over 13.6 eV to 13.6 keV) in the range  $< 300$ . The upper limit on  $\xi$  can be further constrained to  $\xi < 150$ , since for an ionizing continuum such as that observed in NGC 6814, fully stripped Fe (producing no fluorescence) will dominate for  $\xi > 150$  (see Fig. 2). Assuming that the reprocessing gas is optically thick, it will reprocess the continuum radiation and reach an equilibrium at an effective blackbody temperature  $\sim 2 \times 10^5$  K (Begelman & deKool 1991). This temperature of the blackbody is too cool to be observed in the *Ginga* bandpass, but qualitatively it is similar to the soft X-ray excesses observed in other AGNs (cf. Turner & Pounds 1989).

The increase in  $W_\alpha$  with increasing ionization of the material is more pronounced for disk reflection than for the warm absorber, as photons are reflected at the mean optical depth of unity, i.e.,  $N_H \sim 8 \times 10^{23}$   $cm^{-2}$  at the Fe edge (as opposed to  $\sim 2 \times 10^{23}$   $cm^{-2}$ , which was required for the warm absorber). Note that this value of  $N_H$  is roughly independent of the ionization state of Fe because of the small change of the Fe cross section over the range of ionization states (see, e.g., George & Fabian 1991). For a disk ionized such that iron remains below Fe XVIII (so the line is not required to be substantially

TABLE 2  
DISK-LINE FITS FOR NGC 6814

PARAMETER	DISK INCLINATION ANGLE (assumed)		
	0°	45°	70°
Power-law index $\alpha$ .....	$0.40 \pm 0.08$	$0.40 \pm 0.08$	$0.35 \pm 0.07$
Continuum normalization (photons $s^{-1} keV^{-1}$ ) .....	$41.6 \pm 1.5$	$40.7 \pm 1.5$	$35.70 \pm 3.0$
Column density $N_H$ ( $\times 10^{22} cm^{-2}$ ) .....	$3.77 \pm 0.40$	$3.72 \pm 0.40$	$3.35 \pm 0.40$
Line energy (keV) .....	$7.17 \pm 0.11$	$6.22 \pm 0.14$	$5.23 \pm 0.19$
Line amplitude at the peak (photons $s^{-1} keV^{-1}$ ) .....	$0.24 \pm 0.05$	$0.28 \pm 0.05$	$0.21 \pm 0.05$
Line equivalent width (eV) .....	$633^{+150}_{-100}$	$698^{+150}_{-100}$	$998^{+1030}_{-215}$
$\chi^2$ (22 d.o.f.) .....	15.5	17.0	20.0

NOTE.—In these fits we have taken an inner radius of  $3R_s$  and outer radius of  $50R_s$  as the boundaries for the line origin. We have assumed a power-law dependence of  $-3$  for the emissivity function and used line profile calculations from a relativistic disk (Fabian et al. 1989). Errors are 90% confidence for one interesting parameter.

redshifted), the decrease in opacity leads to an increase in the line of a factor 1.5 (see Fig. 2 of Lightman & White 1988), and the increase in fluorescent yield with ionization state gives a further factor of 1.26. The total increase in the line width is then a factor of 1.9, increasing the expected equivalent width from 177 eV (flat, face-on, cold accretion disk) to 336 eV, not enough to account for the measured diskline equivalent width of 770 eV.

For a highly ionized disk ( $\xi = 100$ ),  $\sim 3.8$  times more photons escape at the line energy for reflection than for a cold disk (see Fig. 2 of Lightman & White 1988). However, at the line energy, only  $\sim 10\%$  of the incident continuum is reflected, resulting in an increase in the observed (direct plus reflected) continuum of only a factor of  $\sim 1.3$ . This leads to a net increase in line equivalent width by a factor of  $\sim 3$ . This, combined with the increased fluorescence yield from Fe XXIV, results in a *maximum* total increase of  $W_\alpha$  by a factor of  $\sim 6$  over that produced from cold material. *We thus conclude that a highly ionized reprocessor can easily explain the observed Fe K $\alpha$  line strength, though its energy is required to be substantially redshifted.*

### 3.4.2. Reflection Spectrum from an Accretion Disk

Fitting a cold disk reflection model (excluding predicted Fe K $\beta$  and Ni K $\alpha$  lines) to the high state data for NGC 6814 gives low values for solid angle of reprocessing component (Turner et al. 1991), even at high inclination angles (where the projected reprocessing surface is smaller by a factor of  $\cos \theta$ ), primarily due to the lack of apparent edge in the data. Ionization of this simple disk (described in more detail in Done et al. 1992a) predicts an even greater iron edge, thus constraining the solid angle to even smaller values. *Such solid angles are inconsistent with the observed line strength, requiring a rejection of these models.*

However, there is an independent indication that disk reprocessing is indeed occurring in these data. A cross-correlation of the 7–20 keV flux with the 3–5.5 keV flux indicates that 20%–50% of the flux in the 7–20 keV band is lagged by 50–200 s, i.e., is reprocessed, as expected from an accretion disk (Done et al. 1991b), and therefore we expect that the line arises in an accretion disk and so is described by the disk-line profile

with  $W_\alpha \sim 776$  eV (cf. § 3.2). That leads to predicted equivalent widths of  $\sim 88$  eV and 40 eV for Fe K $\beta$  and Ni K $\alpha$ , respectively. The inclusion of these lines makes accretion disk fits acceptable, thus allowing reprocessing models to be viable.

In Table 3 we fit a disk reflection spectrum plus Fe K $\alpha$ , K $\beta$ , and Ni K $\alpha$  lines. We approximate the line profiles as broad Gaussians with a common intrinsic width instead of the expected disk-line (as in § 3.4.1), but in the following discussion, we use the equivalent width derived from the disk-line fits. Note that there are no additional free parameters required as the line energies are fixed, and the line widths and intensities are tied to that of the Fe K $\alpha$  line. The simple fit (Table 1) suggests a redshift of 2% for an Fe K $\alpha$  line originating in neutral material. Thus for the cold case, the line energies are fixed at 6.3 keV, 6.94 and 7.35 keV, respectively. The inclusion of Fe K $\beta$  and Ni K $\alpha$  lines increases the predicted flux in the regime of the iron edge; when convolved with the proportional counter response, these features become unresolvable. Hence the allowed solid angle is increased (Table 3). *However, the large iron K $\alpha$  line equivalent width is inconsistent with the constraints on the solid angle subtended by the disk and thus the line cannot arise in such a cold disk.*

We now consider a warm disk with  $\xi = 50$ , the limiting ionization state for which the line energies 6.30, 6.94, and 7.35 keV are valid. The constraints on the solid angle subtended by the disk and on the ionization state are now extremely loose, with upper limits (90% confidence)  $\Omega/2\pi < 0.45, 0.64,$  and 1.32 for inclinations of 0°, 45°, and 70° (Table 3). These solid angles would give 88, 120, and 146 eV respectively (for a flat cold disk illuminated by a power law of energy index 0.5, taken from George & Fabian 1991). Multiplying these equivalent widths by a factor of 1.9 from the increases due to ionization of the material (§ 3.3) is still inconsistent with the observed line.

Finally, we consider a highly ionized reprocessing disk in which the predominant state of iron is Fe XXIV, thus increasing the fluorescent yield by a factor of 2. In order to obtain this, we fixed  $\xi = 100$  with corresponding emitted line energies of  $\sim 6.67, 7.7,$  and 7.8 keV, while the edge energy is now  $\sim 8.6$  keV. In order to produce an observed line at 6.3 keV, we now have to infer a strong redshift ( $\sim 6\%$ ) so that the Fe K $\beta$  and Ni K $\alpha$  lines are at  $\sim 7.3$  keV and the edge at  $\sim 8.3$  keV; such a

TABLE 3  
 "DISK REFLECTION" FITS FOR NGC 6814

PARAMETER	ASSUMED IONIZATION PARAMETER		
	0 (cold case)	50 (warm case)	100 (hot case)
Power-law index $\alpha$ .....	$0.52 \pm 0.10$	$0.48 \pm 0.10$	$0.45 \pm 0.10$
Continuum normalization (photons $s^{-1}$ keV) .....	$52.2 \pm 9.1$	$49.1 \pm 9.0$	$47.1 \pm 9.0$
Column density $N_H$ ( $\times 10^{22}$ $cm^{-2}$ ) .....	$4.30 \pm 0.65$	$4.20 \pm 0.60$	$4.10 \pm 0.60$
Line normalization (photons $s^{-1}$ ) .....	$1.06 \pm 0.50$	$0.92 \pm 0.50$	$1.1 \pm 0.40$
Intrinsic line width $\sigma_{line}$ (keV) .....	$0.33^{+0.20}_{-0.33}$	$0.20^{+0.4}_{-0.2}$	$0.30^{+0.3}_{-0.3}$
Subtended solid angle $\Omega/2\pi$ (sr) for:			
Inclination = $0^\circ$ .....	0.27 (0–0.95)	0.11 (0–0.45)	0.0 (0–0.35)
Inclination = $45^\circ$ .....	0.38 (0–1.34)	0.16 (0–0.64)	0.0 (0–0.49)
Inclination = $70^\circ$ .....	0.79 (0–2.78)	0.32 (0–1.32)	0.0 (0–1.02)
$\chi^2$ (20 d.o.f.) .....	13	14	14

NOTES.—In these fits we have assumed that the reprocessor is exposed to 100% of the continuum flux. For the neutral (cold) case ( $\xi = 0$ ), the Fe  $K\alpha$  line energy is frozen at 6.3 keV (2% gravitational redshift), so the corresponding lines for Fe  $K\beta$  and Ni  $K\alpha$  are frozen at 6.94 and 7.35 keV, respectively. For the warm case ( $\xi = 50$ ), the line energies are as for the cold case, as this ionization state does significantly increase the line energies (see Fig. 2). For the hot case ( $\xi = 100$ ), the line energies are significantly different than those for neutral or warm material; the combined effects of ionization and gravitational redshift result in a blend of Ni  $K\alpha$  and Fe  $K\beta$  at  $\sim 7.35$  keV, while Fe  $K\alpha$  is at 6.3 keV. Errors are 90% confidence for one interesting parameter.

redshift can only be produced in disk-line models with inclinations  $< 35^\circ$ , as for higher inclinations, the Doppler blueshift dominates over the gravitational redshift (see, e.g., Matt, Perola, & Stella 1992). Fitting such a model, we once again get tighter constraints on the disk solid angle,  $\Omega/2\pi < 0.35$ , 0.49, and 1.02 for inclinations of  $0^\circ$ ,  $45^\circ$ , and  $70^\circ$  (Table 3). This is because the Fe  $K\beta$  and Ni  $K\alpha$  lines are no longer providing photons which will fill in the iron edge (the edge energy being more sensitive to increased ionization than the line energies; see Fig. 2). For a cold disk, these solid angles imply equivalent widths of 61, 85, and 102 eV, respectively, but the maximum total increase of a factor of 6 (from ionization effects) gives an implied equivalent width of  $\sim 500$  eV (for  $45^\circ$ ), still not quite consistent with the diskline fits (see Table 2).

However, the reflection spectrum can be depressed without affecting the line by increasing the abundances of all the elements (George & Fabian 1991, Fig. 17). While the number of line-emitting photons is increased (from an increase in Fe), so is the opacity at the line energy (from the increase in elements such as C, N, and O). These two effects almost completely cancel out in the resultant equivalent width of the line. However, the increase in disk opacity reduces the reflection probability, and hence the normalization of the reflection spectrum. The solid angle subtended by the disk also affects the reflection spectrum normalization, so these two physically distinct effects can both be described simply by the normalization: thus a flared disk ( $\Omega/2\pi \sim 1.5$ ) of 3 times solar abundance would have a reflection spectrum normalization equivalent to that of a solar abundance disk which only subtends a solid angle of  $\Omega/2\pi \sim 0.5$ .

A very narrow funnel is unlikely, so we restrict discussion to a solid angle  $\Omega/2\pi < 1.5$ . For a warm disk ( $\xi = 50$ ), this limit on the solid angle for reflection allows at most 3 times solar abundance, not enough to account for the observed line. However, for the highly ionized disk at  $45^\circ$ – $0^\circ$ , a 1.4–2 times solar abundance can provide a consistent solution for the

intense iron line and reflection spectrum. We show the consistent solution for a highly ionized disk (inclined at  $45^\circ$ ,  $\Omega/2\pi = 0.7$ , abundance = 1.4 times solar) in Figures 5a–5c, but note that the Fe  $K\alpha$  line energy is required to be redshifted.

We suggest that the other strong iron  $K\alpha$  line sources, i.e., Mrk 841 (Day et al. 1990), MCG –5-23-16 (Piro 1991), and 3C 382 (Kaastra, Kunieda, & Awaki 1991), which show similar flat X-ray spectra but apparently no strong reprocessing component in the *Ginga* data, may indeed have a strong ionized reprocessed component, but with the iron edge filled in with photons from other strong lines. Although the expected intrinsic line energy from ionized material is  $> 6.4$  keV, the fact that the observed energy of iron K lines in these Seyfert galaxies is consistent with  $\sim 6.4$  keV is not implausible. As the density of the disk increases monotonically outward (in most viscosity parameterizations), the ionization parameter is a strongly decreasing function of radius. Thus the region in which the intrinsic line energy is  $> 6.4$  keV is strongly concentrated toward the smallest radii where the gravitational redshift effects will be most important. For example, for a face-on disk with viscosity proportional to total pressure (giving  $n \propto r^{1.5}$ ), the ionization of the disk can then be parameterized as  $\xi = \xi_0 (r/3)^{-3.5}$ , where  $r$  is in Schwarzschild radii and  $\xi_0$  describes the ionization state at the inner edge of the disk. The logarithmically weighted mean line energy (integrated between  $3 < r < 1000$ ), including the effects of gravitational and transverse redshift [ $E/E_0 = (1 - 1/r)^{1/2}(1 - 1/2r)^{1/2}$ ], from the face-on disk is then 6.33 keV for  $\xi_0$  of 1000, as opposed to 6.26 keV for  $\xi_0 = 1$ .

There are other effects which may be important in reducing the observed edge in NGC 6814. Both Doppler motions and Compton scattering will smear the edge and line together. However, the edge is more affected by this as it is an intrinsically broad feature, unlike the line. The effects of Doppler broadening and Comptonization in a hot accretion disk corona are discussed in Matt et al. (1991) and Czerny &

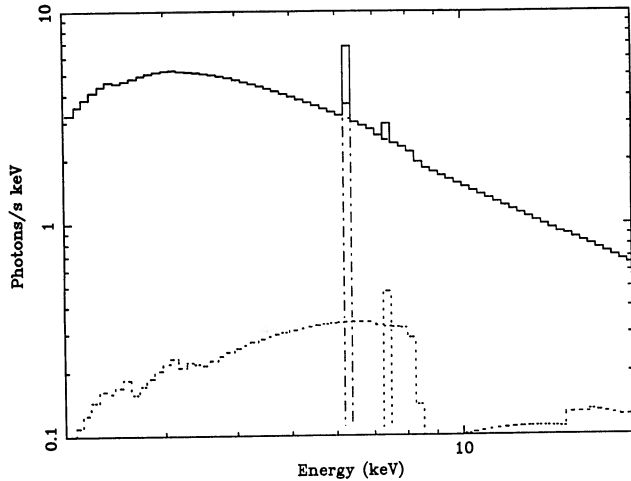


FIG. 5a

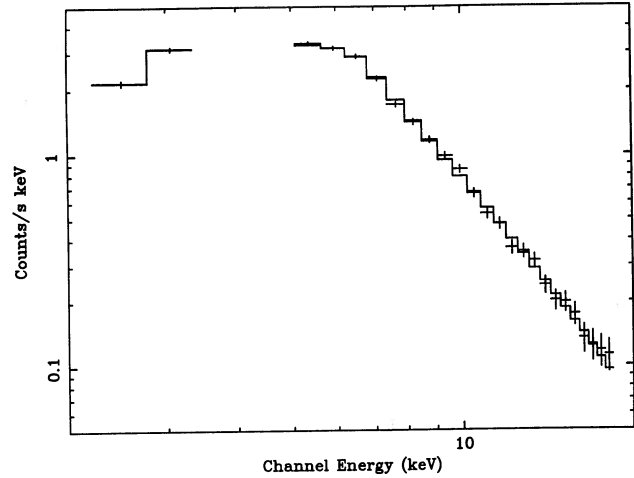


FIG. 5b

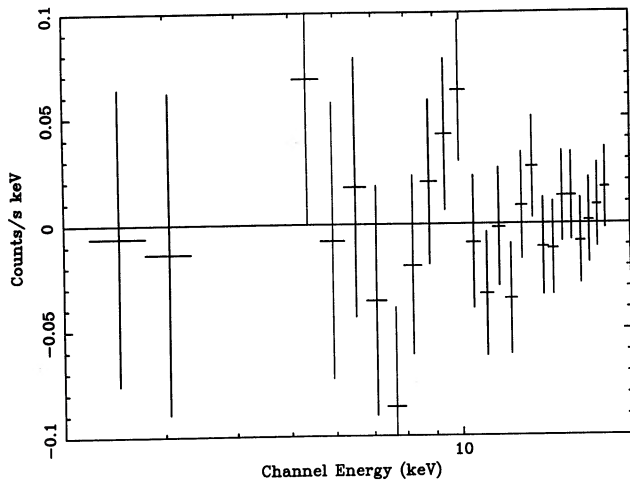


FIG. 5c

FIG. 5.—(a) The self-consistent model in which the Fe  $K\alpha$  line with equivalent width of 770 eV is produced from a highly ionized disk ( $\xi = 100$ ) of  $1.4 \times$  solar abundance subtending a solid angle of  $\Omega/2\pi = 0.7$  to the X-ray source and inclined at  $45^\circ$  to the observer. Fe  $K\beta$  and Ni  $K\alpha$  lines are included as given in Table 3. See the text for details. (b) The *Ginga* data for NGC 6814 and the preferred model (as illustrated in [a]), folded through the detector response. (c) The residuals to the model illustrated in (a).

Zbyszewska (1991). Differences in the angular distribution of the line and edge from a disk can also work to suppress the edge.

The confirmation of the  $\sim 12,000$  s period in the *Ginga* timing data (Done et al. 1992b; see also Done et al. 1991a, b) leads us to a refinement of the above model. We hypothesize that the periodic component in the data is due to periodic partial occultation of both the primary and reprocessed emission by the ragged edge of a geometrically and optically thick rotating accretion disk. The stability of such a ragged disk edge has already been established in numerical simulations by Hawley (1990). The suggestion by Kaastra et al. (1991) that high equivalent width sources are typically highly inclined is consistent with the disk occultation scenario for NGC 6814. This may be reconciled with the low ( $< 35^\circ$ ) inclination required by the disk-line fits as the disk postulated here is no longer flat.

#### 4. CONCLUSIONS

*Ginga* observations of NGC 6814 reveal a complex and variable X-ray spectrum. There is spectral variability below 4 keV, a strong iron line, yet very little evidence for an associated iron edge. The low-energy spectral variability can be explained by the presence of a warm absorber in the system, giving the anticorrelation of  $N_{\text{H}}$  with intensity due to the changing opacity of low-Z elements (mainly oxygen). However, the column density inferred from the upper limit to the Fe edge is insufficient to produce the  $\sim 350$  eV equivalent width Gaussian line in all conditions except those of a highly ionized absorber. Such an ionized scenario, however, cannot explain the spectral variability behavior, as oxygen is completely stripped, so additional cooler material must also be present in the line of sight, requiring a more detailed model with density and ionization stratification and fully self-consistent radiative transfer.

An alternative origin for the line is in an accretion disk, where the ordered angular momentum structure imparts a characteristic profile to the line. Fitting this profile increases the observed equivalent width to  $\sim 770$  eV. Such a large line can be obtained from disk fluorescence only if the reprocessing material is highly ionized, where the enhanced photon escape and increased fluorescence yield can boost the equivalent width by up to a factor of 6.

The apparent inconsistency between the solid angle required to produce the Fe  $K\alpha$  line and the upper limit on solid angle for the Compton reflection component is resolved by allowing the material to be ionized (and including the strong predicted Fe  $K\beta$  and Ni  $K\alpha$  lines in the model), and by postulating a moderate increase in elemental abundances. Similar models may well explain the X-ray spectra of other strong iron line sources such as Mrk 841, MCG -5-23-16, and 3C 382, where fine-tuning of the line energy is not required as the effects of ionization are naturally cancelled by gravitational redshift.

We have discussed the spectral data in terms of two currently popular models for the distribution of matter around the black hole, namely a uniform spherical distribution and an accretion disk. In both cases we require that the material be ionized, as independently postulated in a model by Hayakawa (1991), in which the line is produced in optically thin clumps of material distributed in a thick torus around the black hole.



Since these clumps are optically thin and out of the line of sight, there is no Fe K edge from either reflection or partial covering, so we are unable to rule out this model from the data. However, we prefer the ionized accretion disk scenario discussed here as it allows NGC 6814 to be interpreted in the context of current understanding of other AGNs rather than requiring a completely different accretion structure. All of these

models require an additional, partially ionized absorber in the line of sight to produce the spectral variability below 4 keV.

We thank Tim Kallman for many useful discussions and for providing some of the material for Figure 2. We also thank Keith Jahoda, Julian Krolik, and the anonymous referee for helpful comments.

## REFERENCES

- Bambynek, W., Craseman, B., Fink, R. W., Freund, H.-U., Mark, H., Swift, C. D., Price, R. E., & Rao, P. V. 1972, *Rev. Mod. Phys.*, 44, 716
- Begelman, M. C., & deKool, M. 1991, in *Variability of Active Galactic Nuclei*, ed. H. Miller & P. Wiita (Cambridge: Cambridge Univ. Press), 198
- Czerny, B., & Zbyszewska, M. 1991, *MNRAS*, 249, 634
- Day, C. S. R., Fabian, A. C., George, I. M., & Kunieda, H. 1990, *MNRAS*, 247, 15P
- Done, C., Koyama, K., Kunieda, H., Madejski, G., Mushotzky, R., & Turner, T. J. 1991a, in *IAU Colloq. 129, Structure and Emission Properties of Accretion Disks*, ed. C. Bertout, S. Collin, J.-P. Lasota, & J. Tran Thanh Van (Gif sur Yvette Cedex: Editions Frontières), 417
- Done, C., Madejski, G. M., Mushotzky, R. F., Turner, T. J., Koyama, K., & Kunieda, H. 1991b, *Proc. of the 28th Yamada Conference Frontiers of X-ray Astronomy*, ed. Y. Tanaka & K. Koyama (Tokyo: Universal Academy Press), submitted
- Done, C., Mulchaey, J., Mushotzky, R. F., & Arnaud, K. A. 1992a, *ApJ*, submitted
- Done, C., Madejski, G. M., Mushotzky, R. F., Turner, T. J., Koyama, K., & Kunieda, H. 1992b, *ApJ*, submitted
- Elvis, M., Lockman, F., & Wilkes, B. 1989, *AJ*, 97, 777
- Fabian, A. C., Rees, M. J., Stella, L., & White, N. E. 1989, *MNRAS*, 238, 729
- Fiore, F., Massaro, E., & Barone, P. 1992a, *A&A*, in press
- Fiore, F., Perola, G. C., Matsuoka, M., Yamauchi, M., & Piro, L. 1992b, *A&A*, submitted
- George, I. M., & Fabian, A. C. 1991, *MNRAS*, 249, 352
- Guilbert, P. W., & Rees, M. J. 1988, *MNRAS*, 233, 475
- Halpern, J. P. 1984, *ApJ*, 281, 90
- Halpern, J. P., & Oke, J. B. 1986, *ApJ*, 301, 753
- Hawley, J. F. 1990, *ApJ*, 356, 580
- Hayakawa, S. 1991, *Nature*, 351, 214
- Hayashida, K., et al. 1989, *PASJ*, 41, 373
- House, L. L. 1969, *ApJS*, 18, 21
- Inoue, H. 1989, in *Proc. of the 23rd ESLAB Symposium*, ed. J. Hunt & B. Batrick (Paris: ESA Publications), 783
- Jacobs, V. L., & Rozsnyai, B. F. 1986, *Phys. Rev.*, A34, 1
- Kaastra, J., Kunieda, H., & Awaki, H. 1991, *A&A*, 242, 27
- Kikoin, I. K., ed. 1976, *Tables of Physical Quantities* (Moscow: Atomizdat)
- Klapisch, M., Schwob, J. L., Fraenkel, B. S., & Oreg, J. 1977, *J. Opt. Soc. Am.*, 67(2), 148
- Krolik, J. H., & Kallman, T. R. 1987, *ApJ*, 320, L5
- Kunieda, H., Turner, T. J., Awaki, H., Koyama, K., Mushotzky, R. F., & Tsusaka, Y. 1990, *Nature*, 345, 786 (K90)
- Lambert, D. L. 1989, in *Cosmic Abundances of Matter*, ed. C. J. Waddington (New York: AIP), 168
- Laor, A. 1991, in *Lectures Notes in Physics*, 385, *Iron Line Diagnostics in X-Ray Sources*, ed. A. Treves (Berlin: Springer), 205
- Lightman, A. P., & White, T. W. 1988, *ApJ*, 335, 57
- Makino, F., & the ASTRO-C Team 1987, *Ap. Lett. Comm.*, 25, 223
- Makishima, K. 1986, in *The Physics of Accretion onto Compact Objects*, ed. K. O. Mason, M. G. Watson, & N. E. White (Berlin: Springer-Verlag), 249
- Matt, G., Perola, G. C., & Piro, L. 1991, *A&A*, 247, 25
- Matt, G., Perola, G. C., & Stella, L. 1992, *A&A*, submitted
- Mittaz, J. P. D., & Branduardi-Raymont, G. 1989, *MNRAS*, 238, 1029
- Morita, S., & Fujita, J. 1983, *J. Phys. Soc. Japan*, 52(6), 1957
- Morrison, R., & McCammon, D. 1983, *ApJ*, 270, 119
- Piro, L. 1991, *Proc. of the 28th Yamada Conference, Frontiers of X-ray Astronomy*, ed. Y. Tanaka & K. Koyama (Tokyo: Universal Academy Press), submitted
- Pounds, K. A., Nandra, K. P., Stewart, G. C., George, I. M., & Fabian, A. C. 1990, *Nature*, 344, 132
- Rielman, R. F., & Manson, S. T. 1979, *ApJS*, 40, 815
- Shakura, N. I., & Sunyaev, R. A. 1973, *A&A*, 24, 337
- Tennant, A. F., Mushotzky, R. F., Boldt, E. A., & Swank, J. H. 1981, *ApJ*, 251, 15
- Turner, M. J. L., et al. 1989, *Proc. Astr. Soc. Japan*, 41, 35
- Turner, T. J., Done, C., Kunieda, H., Mushotzky, R. F., & Awaki, H. 1991, in *IAU Colloq. 129, Structure and Emission Properties of Accretion Disks*, ed. C. Bertout, S. Collin, J.-P. Lasota, & J. Tran Thanh Van (Gif sur Yvette Cedex: Editions Frontières), 545
- Turner, T. J., & Pounds, K. A. 1989, *MNRAS*, 240, 833